

## LETTERS

# Effect of evaporite deposition on Early Cretaceous carbon and sulphur cycling

Ulrich G. Wortmann<sup>1</sup> & Boris M. Chernyavsky<sup>1</sup>

The global carbon and sulphur cycles are central to our understanding of the Earth's history, because changes in the partitioning between the reduced and oxidized reservoirs of these elements are the primary control on atmospheric oxygen concentrations. In modern marine sediments, the burial rates of reduced carbon and sulphur are positively coupled, but high-resolution isotope records indicate that these rates were inversely related during the Early Cretaceous period<sup>1</sup>. This inverse relationship is difficult to reconcile with our understanding of the processes that control organic matter remineralization and pyrite burial. Here we show that the inverse correlation can be explained by the deposition of evaporites during the opening of the South Atlantic Ocean basin. Evaporite deposition can alter the chemical composition of sea water<sup>2,3</sup>, which can in turn affect the ability of sulphate-reducing bacteria to remineralize organic matter and mediate pyrite burial. We use a reaction–transport model to quantify these effects, and the resulting changes in the burial rates of carbon and sulphur, during the Early Cretaceous period. Our results indicate that deposition of the South Atlantic evaporites removed enough sulphate from the ocean temporarily to reduce biologically mediated pyrite burial and organic matter remineralization by up to fifty per cent, thus explaining the inverse relationship between the burial rates of reduced carbon and sulphur during this interval. Furthermore, our findings suggest that the effect of changing seawater sulphate concentrations on the marine subsurface biosphere may be the key to understanding other large-scale perturbations of the global carbon and sulphur cycles.

The global cycling of sulphur (S) is controlled by the balance of S entering the ocean as a result of weathering, volcanic activity and hydrothermal fluxes, and the removal of S from the ocean in the form of S-bearing sediments. Oxidation of reduced S species consumes oxygen and forms dissolved sulphate, which is subsequently returned to the sedimentary reservoir in its oxidized form as CaSO<sub>4</sub>, or it is reduced by bacterial activity and exported as pyrite. An increase of the pyrite oxidation rate relative to the pyrite burial rate therefore results in the net loss of atmospheric oxygen, and vice versa. A similar reasoning applies to carbon (C), which enters the sedimentary reservoir either as oxidized C (carbonate) or as reduced C (organic matter). However, sulphate reduction (pyrite production) is achieved by a microbially mediated redox reaction requiring the presence of organic matter as an electron donor. Because the capacity of most marine sediments to form pyrite is limited by organic-matter availability and not sulphate supply<sup>4</sup>, perturbations to either the reduced C or reduced S flux are positively coupled to the other. As the microbially mediated reduction of C and S involves a considerable negative isotope effect (up to –70‰ for S, and about –28‰ for C; refs 5–8), an increase in the burial rate of the reduced species relative to the oxidized species results in a positive shift of the isotopic ratio, and vice versa. This allows us to trace the behaviour of the C and S cycles through Earth's history.

High-resolution  $\delta^{34}\text{S}$  and  $\delta^{13}\text{C}$  records<sup>1</sup> show that during the Early Cretaceous a large negative  $\delta^{34}\text{S}$  excursion is accompanied by a large positive  $\delta^{13}\text{C}$  excursion<sup>9,10</sup>. This implies that decreased pyrite burial rates occur together with increased organic-matter burial rates (we note that it is irrelevant whether this was caused by increased organic-matter production or increased organic-matter preservation). Previous studies explained this paradox by suggesting a global iron deficiency<sup>11</sup>, or a global shift of organic-matter burial from the ocean to sulphate-limited continental settings<sup>4</sup>. Both scenarios seem unlikely during the Early Cretaceous, because the existing marine data clearly show increased organic-matter content or even black shale deposition<sup>12,13</sup>, and there is little evidence to support reduced iron availability, or a shift of organic-matter deposition to terrestrial environments. A recent study suggested changes in volcanic and hydrothermal activity, together with increased weathering and reduced pyrite burial fluxes<sup>1</sup>, to increase the flux of isotopically light S. However, this would also increase the flux of isotopically light C, and thus result in a positive coupling of the  $\delta^{34}\text{S}$  and  $\delta^{13}\text{C}$  signals.

Although it is difficult to explain the Early Cretaceous C–S paradox while assuming a modern ocean chemistry, we note that the Early Cretaceous perturbations of the C and S cycles are contemporaneous with the early stages of the opening of the South Atlantic. The break-up between South Africa and South America resulted in the creation of a silled 10<sup>6</sup> km<sup>2</sup> below-sealevel basin, which existed between 126 and 116 Myr ago<sup>14</sup>. During this time interval, evaporites totalling a volume of 1–4 × 10<sup>15</sup> m<sup>3</sup> were deposited in this basin<sup>14,15</sup>. Assuming that 20% of these evaporites consist of CaSO<sub>4</sub> (refs 16, 17), these deposits contain between 4.4 × 10<sup>18</sup> to 17.6 × 10<sup>18</sup> mol CaSO<sub>4</sub>, equivalent to 26% to 100% of the current seawater sulphate reservoir. Here, we will therefore explore the impact of the South Atlantic evaporite sequences on the global cycling of S and C. We do this by coupling a sediment diagenetical model that describes organic-matter remineralization and pyrite burial as a function of seawater sulphate concentrations to a box model describing the global C and S cycles (see Methods and the Supplementary Information).

Our model captures the magnitude and timing of the marine  $\delta^{13}\text{C}$  and  $\delta^{34}\text{S}$  signals quite well (Figs 1 and 2). However, the magnitude of the  $\delta^{13}\text{C}$  signal depends on the initial marine sulphate concentration: we obtain a positive shift of 3.5‰ assuming a 5 mM ocean, and +2.5‰ shift for 8 mM or 12 mM sulphate concentrations in the ocean (Figs 1 and 2). Depending on the input parameters chosen (an evaporite volume of 4 × 10<sup>15</sup> m<sup>3</sup> and a 5 mM sulphate concentration, versus an evaporite volume of 1 × 10<sup>15</sup> m<sup>3</sup> and 12 mM sulphate concentration), we obtain minimum or maximum estimates suggesting that the South Atlantic evaporites contain between 8% to 63% CaSO<sub>4</sub>. These numbers are not too different from the long-term average gypsum content of evaporitic sequences (20%)<sup>16,17</sup>, and may be affected by the high-calcium and low-sulphate concentrations of

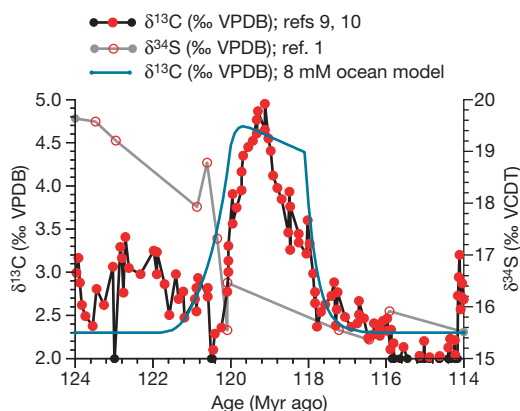


**Figure 1** | A comparison between the observed<sup>9,10</sup>  $\delta^{13}\text{C}$  and the  $\delta^{13}\text{C}$  predicted by our C and S model and the  $\delta^{34}\text{S}$  data<sup>1</sup>. Both magnitude and timing of the Aptian  $\delta^{13}\text{C}$  excursion are well captured by our model. VCDT, Vienna Canyon Diablo Troilite. The numerical ages of the  $\delta^{13}\text{C}$  data are based on ref. 27.

Early Cretaceous ocean water, which favour the precipitation of gypsum over other evaporitic phases<sup>18</sup>.

The post-event shape of the modelled S-isotope data shows a first-order match with the published data (Fig. 2). However, the post-event isotope data depends on the choice of unconstrained post-event evaporite burial rates. It is therefore not possible to decide whether the second-order features visible in the published data are positive or negative excursions from the first-order signal. However, we tentatively relate the first and smallest excursion (112 Myr ago) to the onset of pyrite burial after marine sulphate levels increased sufficiently to sustain significant rates of organic-matter remineralization. The second and largest S-isotope excursion (95 Myr ago) is possibly related to increased pyrite burial rates during the Cenomanian black shale interval (OAE 2)<sup>12,13,19</sup>. However, these second-order features may also be explained by changes in weathering, volcanic and hydrothermal fluxes or changes in sea level<sup>20–22</sup>.

The proposed dramatic changes in the marine sulphate budget must have left their mark on Early Cretaceous sedimentary

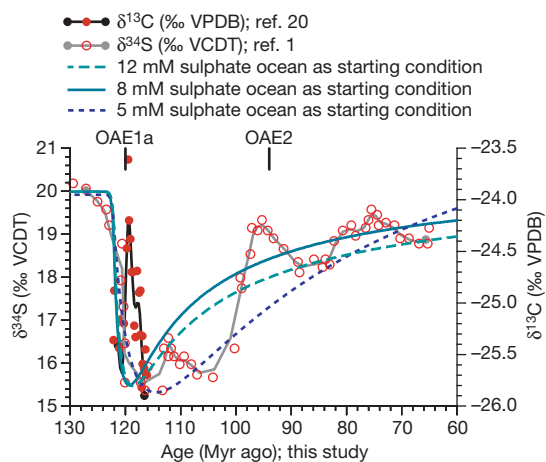


**Figure 2** | Comparison of the published  $\delta^{34}\text{S}$  data<sup>1</sup> and the  $\delta^{13}\text{C}$  data<sup>20</sup> with three different model runs. The dotted line shows the results for a model assuming an initial marine sulphate concentration of 5 mM and a post-event decrease in sulphate burial rate. The solid line shows the result for an ocean with an initial sulphate concentration of 8 mM, in which the post-event sulphate burial rate is similar to the pre-event sulphate burial rate. The dashed line is similar to the 8 mM model, but assumes an ocean with an initial sulphate concentration of 12 mM. Circles represent data points, and the grey line represents a three-point moving average. OAE1a and OAE2 are major oceanic anoxic events.

sequences. We therefore investigated a chemostratigraphically well-dated shale section from the northern Tethyan margin in southern Germany<sup>20,23</sup>. These shales are characterized by a striking black/green cyclicity that records changes in organic-matter content (up to 5%), possibly related to astronomical forcing<sup>23</sup>. The short-term variability in organic-matter content is complemented by a remarkable long-term stability of the overall composition from Early Aptian to Late Albian times. That is, Fe and organic-matter contents do change from a black to a green layer, but if we compare layers of similar colour, major-element and trace-element ratios remain stable. The major exception to this pattern is the S content of the shales, which drops during the Early Aptian within a few million years by an order of magnitude from 0.5 to 0.05 wt%, and remains low for approximately three million years (Fig. 3). This drop is remarkable because it is unrelated to the organic-matter and Fe contents of the sediment. However, the timing of this dramatic reduction of sedimentary S content is coeval with the deposition of evaporites in the South Atlantic.

From these results and the range of published data on the South Atlantic evaporite sequences and Early Cretaceous sulphate concentrations, we conclude that large-scale evaporite depositional events can greatly alter the sulphate concentration of ocean water. These changes can affect the ability of the marine subsurface biosphere to remineralize organic matter and to mediate pyrite formation. This has several important consequences: (1) increased organic-matter burial rates may result in increased  $\text{CO}_2$  drawdown rates; (2) decreased organic-matter remineralization rates must affect the global availability of phosphorus; (3) the drastically reduced sulphate concentrations must affect the ability of sulphate-reducing bacteria to oxidize methane, and thus modulate the global methane flux.

Our findings demonstrate that despite the different residence times of C and S in the ocean ( $10^3$  versus  $10^7$  years), transient perturbations in either cycle must be either positively or negatively coupled to perturbations in the other, the respective magnitudes being a function of seawater sulphate concentrations. Low-sulphate concentrations dominated over most of the last 550 Myr (refs 18, 24,

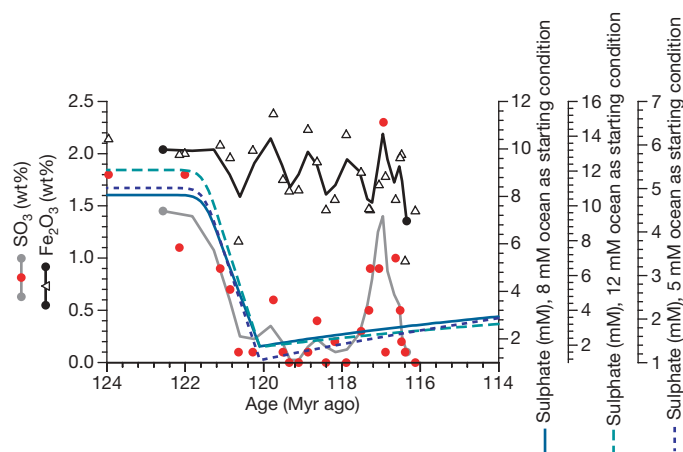


**Figure 3** | Comparison between sedimentary S and Fe contents in an Aptian deep-sea section with model predicted seawater concentrations. In all model runs, the measured S content of the sediments mirrors the sharp decrease of the seawater concentrations. We note that the decreasing S values are not related to a decrease in Fe content. The decoupling between Fe and S is an artefact of the deep marine nature of the sampling site. organic matter in deep marine settings is highly refractory and reduction (and thus  $\text{FeS}_2$  formation) is slow, continuing for millions of years after initial deposition (see ref. 28). Reduced diffusive fluxes therefore greatly alter the location where reduction takes place, shifting the location of  $\text{FeS}_2$  formation. The fluctuations seen in the Fe data are caused by changes in bottom-water oxygenation<sup>23</sup>. The thick solid lines are obtained by processing the original data (circles and triangles) with a three-point moving-average window.

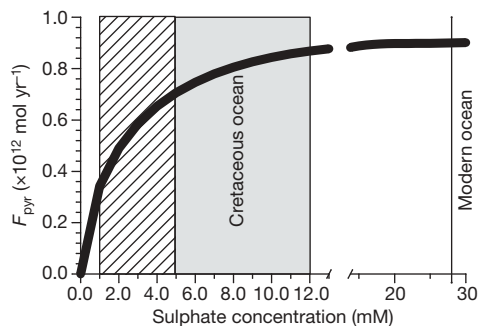


**Figure 4 | Modelled response of the depth-integrated pyrite burial flux in an arbitrary sediment to changing sulphate concentrations at the sediment-water interface.** The grey area shows the range of the published concentration values for Cretaceous ocean water. The hatched area shows the modelled seawater concentration range after the deposition of the South Atlantic evaporite sequences. Note the interrupted sulphate concentration scale.

25), so this interpretation may well be the key to understanding what has been termed the central dilemma of C-S geochemistry<sup>3</sup>.

## METHODS

**Modelled seawater sulphate concentrations.** To characterize the response of the marine subsurface biosphere to changing seawater sulphate concentrations, we use REMAP<sup>26</sup> to solve a reaction transport model describing the sulphate-concentration-dependent bacterial activity using the seawater sulphate concentration as a Dirichlet boundary condition at the upper boundary, and a zero-gradient Neumann condition at the lower boundary. Using this model, we calculate pyrite burial rates as a function of seawater sulphate concentrations (see Fig. 4). The resulting pyrite burial fluxes are scaled to equal the global flux at the given starting conditions of the model. The sulphate-concentration-dependent burial fluxes are now used as input parameters in a box model describing the evolution of the marine  $\delta^{34}\text{S}$  and  $\delta^{13}\text{C}$  values. For the C-cycle model, we assume as a first-order approximation that the remineralization rate is proportional to the pyrite burial rate, which depends on sulphate. We can thus formulate a time-dependent box model in which we relate organic-matter burial to sulphate availability.

**The box model.** For the box model, we assume an ocean volume of  $1.38 \times 10^{18} \text{ m}^3$  (see ref. 14) for all model runs, and present our results for an ocean with initial (that is, pre-event) sulphate concentrations of 5 mM, 8 mM and 12 mM covering the range of the published data<sup>18</sup>. Changes in the input fluxes of the S cycle have already been modelled<sup>1</sup>, so we consider the hydrothermal, volcanic and weathering fluxes as a single and constant source, using a net input flux of  $2 \times 10^{12} \text{ mol yr}^{-1}$  (ref. 1). Using these parameters, the model achieves steady-state conditions for an evaporitic output flux of  $1.1 \times 10^{12} \text{ mol yr}^{-1}$  and a pyritic output flux of  $0.90 \times 10^{12} \text{ mol yr}^{-1}$ . For the isotopic calculation, we use a seawater  $\delta^{34}\text{S}$  of 20‰ (ref. 1), and a  $\delta^{34}\text{S}$  of 5.76‰ for the combined hydrothermal, erosional and volcanic fluxes. The model achieves isotopic equilibrium for a seawater-pyrite difference of  $-31.55\%$ .

**The C-cycle model.** The C-cycle model assumes that the mass of dissolved C in the ocean is  $3.2 \times 10^{18} \text{ mol}$ , and a net input flux of  $25.43 \times 10^{12} \text{ mol C yr}^{-1}$  with a  $\delta^{13}\text{C}$  value of  $-5.98\%$  VPDB (the Vienna Pee-Dee Belemnite standard). The output flux into the oxidized reservoir is kept constant at  $20 \times 10^{12} \text{ mol yr}^{-1}$  and is assumed to happen in isotopic equilibrium. The initial burial flux of organic matter is set at  $5.43 \times 10^{12} \text{ mol yr}^{-1}$  with an isotopic offset of  $-28\%$  relative to the contemporaneous sea water. The combined C- and S-cycle model is then run by perturbing the steady state with a pulsed evaporitic depositional event, where the size of this event is modified until a good fit between predicted and measured S data is achieved. A detailed discussion of the above models and their parameterization is given in the Supplementary Information.

Received 7 April 2006; accepted 21 February 2007.

1. Paytan, A., Kastner, M., Campbell, D. & Thiemens, M. H. Seawater sulfur isotope fluctuations in the Cretaceous. *Science* **304**, 1663–1665 (2004).
2. Arthur, M. A. in *Climate in Earth History* 55–67 (National Academy Press, Washington DC, 1982).
3. Holser, W. T., Schidlowski, M., Mackenzie, F. T. & Maynard, J. B. in *Chemical Cycles in the Evolution of the Earth* 105–174 (John Wiley & Sons, New York, 1988).

4. Berner, R. A. & Raiswell, R. Burial of organic carbon and pyrite sulfur in sediments over phanerozoic time: a new theory. *Geochim. Cosmochim. Acta* **47**, 855–862 (1983).
5. Wortmann, U. G., Bernasconi, S. M. & Böttcher, M. E. Hypersulfidic deep biosphere indicates extreme sulfur isotope fractionation during single step microbial sulfate reduction. *Geology* **29**, 647–650 (2001).
6. Brunner, B. & Bernasconi, S. M. A revised isotope fractionation model for dissimilatory sulfate reduction in sulfate reducing bacteria. *Geochim. Cosmochim. Acta* **69**, 4759–4771 (2005).
7. Deines, P. in *Handbook of Environmental Geochemistry* (eds Fritz, P. & Fontes, J. C.) Vol. 1, 239–406 (Elsevier, New York, 1980).
8. O’Leary, M. H. Carbon isotope fractionation in plants. *Phytochemistry* **20**, 553–567 (1981).
9. Herrle, J. O., Köbller, P., Friedrich, O., Erlenkeuser, H. & Hemleben, C. High-resolution carbon isotope records of the Aptian to Lower Albian from SE France and the Magazan Plateau (DSDP Site 545): a stratigraphic tool for paleoceanographic and paleobiologic reconstruction. *Earth Planet. Sci. Lett.* **218**, 149–161 (2004).
10. Erba, E. et al. Integrated stratigraphy of the Cismon Apticore (Southern Alps, Italy): A ‘reference section’ for the Hauterivian-Aptian interval at low latitudes. *J. Foraminiferal Res.* **29**, 371–391 (1999).
11. Raiswell, R. & Canfield, D. E. Sources of iron for pyrite formation in marine sediments. *Am. J. Sci.* **298**, 219–245 (1988).
12. Ryan, W. B. F. & Cita, M. B. Ignorance concerning episodes of ocean-wide stagnation. *Mar. Geol.* **23**, 197–215 (1977).
13. Schlanger, S. O. & Jenkyns, H. C. Cretaceous oceanic anoxic events: causes and consequences. *Geol. Mijnbouw* **55**, 179–184 (1976).
14. Burke, K. & Sengör, C. Ten metre global sea-level change associated with South Atlantic Aptian salt deposition. *Mar. Geol.* **83**, 309–312 (1988).
15. Southam, J. R. & Hay, W. W. in *The Oceanic Lithosphere* (ed. Emiliani, E.) Vol. 7 of *The Sea* 1617–1684 (Wiley-Interscience, New York, 1981).
16. Zharkov, M. A. *History of Paleozoic Salt Accumulation* 1–308 (Springer, New York, 1981).
17. Rhonov, A. B. The earth’s sedimentary shell (quantitative patterns of its structure, compositions, and evolution). *Int. Geol. Rev.* **24**, 1365–1388 (1982).
18. Lowenstein, T. K., Hardie, L. A., Timofeev, M. N. & Demicco, R. V. Secular variation in seawater chemistry and the origin of calcium chloride basinal brines. *Geology* **31**, 857–860 (2003).
19. Arthur, M. A. & Premoli Silva, I. in *Nature and Origin of Cretaceous Carbon-Rich Facies* (eds Schlanger, S. O. & Cita, M. B.) 7–54 (Academic, San Diego, California, 1982).
20. Wortmann, U. G., Herrle, J. O. & Weissert, H. Altered carbon cycling and coupled changes in Early Cretaceous weathering patterns: Evidence from integrated carbon isotope and sandstone records of the western Tethys. *Earth Planet. Sci. Lett.* **220**, 69–82 (2004).
21. Weissert, H. & Erba, E. Volcanism, CO<sub>2</sub> and paleoclimate: A Late Jurassic-Early Cretaceous carbon and oxygen isotope record. *J. Geol. Soc.* **161**, 695–702 (2004).
22. Bjerrum, C. J., Bendtsen, J. & Legarth, J. J. F. Modeling organic carbon burial during sea level rise with reference to the Cretaceous. *Geochem. Geophys. Geosyst.* **7**, Q05008, doi:10.1029/2005GC001032 (2006).
23. Wortmann, U. G., Zacher, W. & Hesse, R. Major-element data from cyclic black shales and their paleoceanographic implications for the early Cretaceous deep western Tethys. *Paleoceanography* **14**, 525–541 (1999).
24. Berner, R. A. A model for calcium, magnesium and sulfate in seawater over phanerozoic time. *Am. J. Sci.* **304**, 438–453 (2004).
25. Holland, H. D. Sea level, sediments and the composition of seawater. *Am. J. Sci.* **305**, 220–239 (2005).
26. Chernyavsky, B. & Wortmann, U. G. REMAP: A reaction transport model for isotope ratio calculations in porous media. *Geochem. Geophys. Geosyst.* **8**, Q02009, doi:10.1029/2006GC001442 (2006).
27. Leckie, R. M., Bralower, T. J. & Cashman, R. Oceanic anoxic events and plankton evolution: Biotic response to tectonic forcing during the mid-Cretaceous. *Paleoceanography* **17**, 1–29 doi:10.1029/2001PA000623 (2002).
28. Parkes, R. J. et al. Deep sub-seafloor prokaryotes stimulated at interfaces over geological time. *Nature* **436**, 390–394 (2004).

**Supplementary Information** is linked to the online version of the paper at [www.nature.com/nature](http://www.nature.com/nature).

**Acknowledgements** We thank M. Kastner, B. Hay, H. Weissert, N. Andersen, A. J. M. Stams and B. Brunner for discussions. J. Bollmann, E. T. C. Spooner, J. Walker, L. Lee, J. Yap and C. Banks provided helpful comments on an earlier version of this manuscript. We gratefully acknowledge the comments of M. Arthur, M. Gorton, H. Li and C. Greybe provided assistance in the laboratory. C. Marra participated in this study as part of a University of Toronto mentorship program for gifted high school students. This work was supported by the Natural Sciences and Engineering Research Council of Canada (NSERC).

**Author Information** Reprints and permissions information is available at [www.nature.com/reprints](http://www.nature.com/reprints). The authors declare no competing financial interests. Correspondence and requests for materials should be addressed to U.G.W. ([uli.wortmann@utoronto.ca](mailto:uli.wortmann@utoronto.ca)).